

The dimensionality of color vision in carriers of anomalous trichromacy

Gabriele Jordan

Institute of Neuroscience, Newcastle University,
Newcastle upon Tyne, UK



Samir S. Deeb

Departments of Medicine and Genome Sciences,
University of Washington, Seattle, USA



Jenny M. Bosten

Department of Experimental Psychology, University of
Cambridge, Cambridge, UK



J. D. Mollon

Department of Experimental Psychology, University of
Cambridge, Cambridge, UK



Some 12% of women are carriers of the mild, X-linked forms of color vision deficiencies called “anomalous trichromacy.” Owing to random X chromosome inactivation, their retinæ must contain four classes of cone rather than the normal three; and it has previously been speculated that these female carriers might be tetrachromatic, capable of discriminating spectral stimuli that are indistinguishable to the normal trichromat. However, the existing evidence is sparse and inconclusive. Here, we address the question using (a) a forced-choice version of the Rayleigh test, (b) a test using multidimensional scaling to reveal directly the dimensionality of the participants’ color space, and (c) molecular genetic analyses to estimate the X-linked cone peak sensitivities of a selected sample of strong candidates for tetrachromacy. Our results suggest that most carriers of color anomaly do not exhibit four-dimensional color vision, and so we believe that anomalous trichromacy is unlikely to be maintained by an advantage to the carriers in discriminating colors. However, 1 of 24 obligate carriers of deuteranomaly exhibited tetrachromatic behavior on all our tests; this participant has three well-separated cone photopigments in the long-wave spectral region in addition to her short-wave cone. We assess the likelihood that behavioral tetrachromacy exists in the human population.

Keywords: color vision, psychophysics, human, tetrachromacy, anomalous trichromacy

Citation: Jordan, G., Deeb, S. S., Bosten, J. M., & Mollon, J. D. (2010). The dimensionality of color vision in carriers of anomalous trichromacy. *Journal of Vision*, 10(8):12, 1–19, <http://www.journalofvision.org/content/10/8/12>, doi:10.1167/10.8.12.

Introduction

Normal human color vision is mediated by three classes of retinal cone, which have peak sensitivities in the short-wave (S), middle-wave (M), and long-wave (L) regions of the spectrum, but 6% of men exhibit a mild deficiency of color vision called “anomalous trichromacy,” in which either the M- or the L-cone sensitivity is thought to be displaced in its spectral position (DeMarco, Pokorny, & Smith, 1992; Hayashi, Motulsky, & Deeb, 1999; Mollon, 1997; Nathans, Piantanida, Eddy, Shows, & Hogness, 1986; Rayleigh, 1881). In the most common case of “deuteranomaly,” affecting 5% of men, the M photopigment is replaced by one closer to L, and in “protanomaly,” affecting 1% of men, the L photopigment is replaced by one closer to M. Intriguingly, the mother (or daughter) of an anomalous trichromat is a candidate for tetrachromacy: on one of her X chromosomes, such a heterozygote has the genes for the normal L- and M-cone photopigments, but on her other she will have, say, a gene for the normal

L photopigment and a gene for the spectrally shifted hybrid photopigment (L') that her anomalous son inherits (see Figures 1A and 1B). Owing to random X chromosome inactivation, only one or other of her two X chromosomes will be expressed in any given cone cell in her retina (Lyon, 1961; Teplitz, 1965). Thus, she will have a retinal mosaic containing four types of cone (see Figure 1C).

But does her visual system have enough plasticity to take advantage of the input from an extra class of cone? Would not a special neural apparatus need to evolve before color vision became four-dimensional? Two animal models suggest that no additional neural mechanism may be necessary. First, although the males of nearly all New World primate species are dichromatic, having an autosomal S-photopigment gene and a single, polymorphic, X-linked photopigment gene, two thirds of the females, heterozygous at the latter locus, become functional trichromats (Mollon, Bowmaker, & Jacobs, 1984). Second, and perhaps more remarkably, some heterozygous knock-in mice expressing the human L photopigment as well as the native mouse M photopigment become trichromatic, exhibiting wavelength

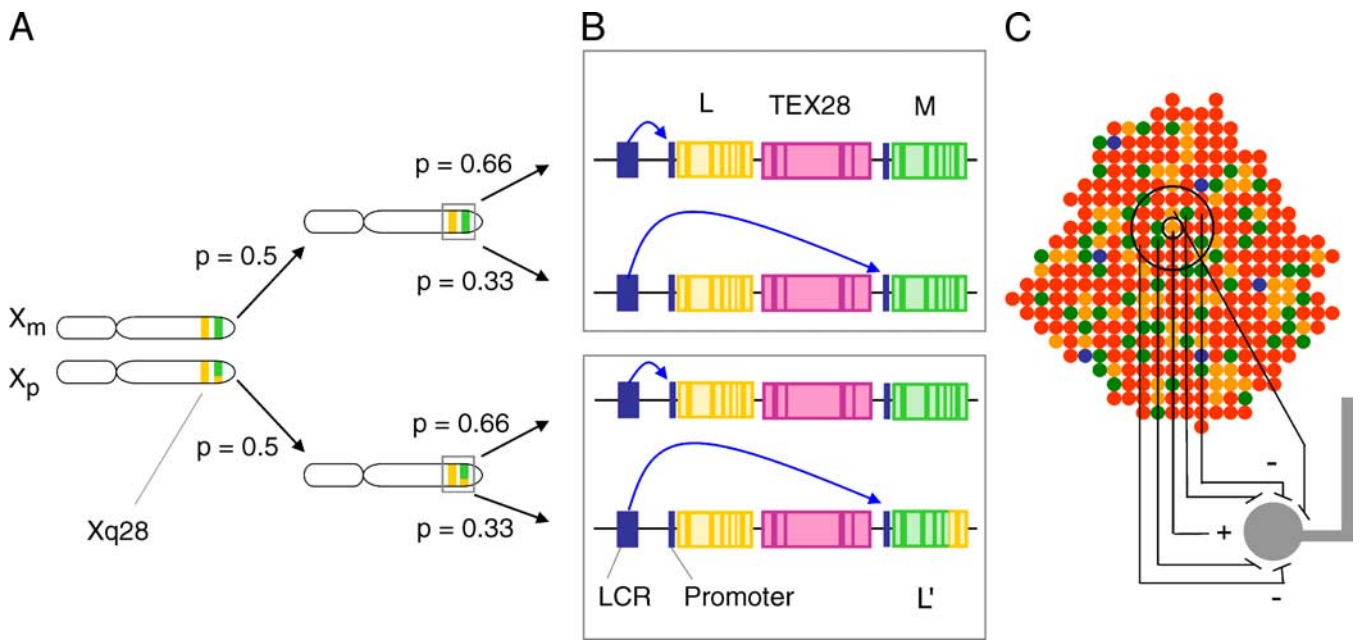


Figure 1. Two stochastic events in succession determine the distribution of cones in the retina of a carrier of anomalous trichromacy. (A) Random X-chromosome inactivation determines whether the maternal (X_m) or the paternal X chromosome (X_p) is expressed within a given cell. The hybrid gene on X_p is indicated by a green-orange band. (B) The binding of an upstream locus control region (LCR) to the promoter region of the first or second opsin gene determines which photopigment is expressed in the cell. There is a bias in favor of the first gene in the array. The more saturated bands in the diagram represent exons. TEX28 is an interposed non-opsin gene. (C) The hypothetical distribution of four cone types in the heterozygous retina: blue, short-wave; green, middle-wave; red, long-wave and orange, hybrid. Superposed on the array is the receptive field of a midget ganglion cell that draws its center input from a single hybrid cone and an opposed surround input from all M, L and L' cones.

discrimination in the red-green region of the spectrum (Jacobs, Williams, Cahill, & Nathans, 2007).

In the case of heterozygous women, as in that of New World monkeys, the neural basis for any enhanced color discrimination is likely to be the midget class of retinal ganglion cells (Mollon et al., 1984). In the fovea, such ganglion cells draw their center input from a single cone (Dacey, 1999). If the surround input is drawn indiscriminately from all (non-S) cones (Lennie, Haake, & Williams, 1991), then the ganglion cell will automatically become chromatically specific (see Figure 1C). We then need only to suppose that the cortex, by Hebbian learning (Linsker, 1990), is able to segregate the signals that originate in the L, M, and “anomalous” cones of the potential tetrachromat (Jordan & Mollon, 1993; Mollon et al., 1984). However, in modeling work, Wachtler, Doi, Lee, and Sejnowski (2007) have suggested that there is insufficient information in natural scenes to allow unsupervised learning of signals specific to a fourth cone type.

It was De Vries (1948, p. 380) who first suggested that carriers of anomalous trichromacy should be tetrachromatic, but the existing evidence supports only *weak tetrachromacy* (Jordan & Mollon, 1993; Nagy, MacLeod, Heyneman, & Eisner, 1981). In weak tetrachromacy, as defined by Jordan and Mollon (1993), there are four types

of cone but only three post-receptoral signals. Such subjects may reveal themselves by a failure of Grassmann’s Third Law of Color Mixing (MacLeod, 1985). The evidence for strong tetrachromacy—where four independent cone signals are available for cortical transformations—is still elusive.

In the present study, we first obtained classical Rayleigh matches for a population of obligate carriers of anomalous trichromacy and their sons. We then used two tests specifically designed to detect behavioral tetrachromacy in the carriers. The first was a discrimination test of lights in the Rayleigh region. The second was a multidimensional scaling test specially developed to reveal the extra dimension of color space expected to exist in the carriers of deuteranomaly. Finally, we used molecular genetic analyses to identify the λ_{\max} values of our carriers’ middle- to long-wave photopigments.

Rayleigh matches

In selecting participants, our strategy was first to identify boys who are anomalous trichromats. We predicted that the most plausible candidates for strong

tetrachromacy would be the mothers of those boys who had small matching ranges on a clinical anomaloscope: it is thought that precision in color matching indicates good spectral separation of the underlying photopigments (Regan, Reffin, & Mollon, 1994; Shevell, He, Kainz, Neitz, & Neitz, 1998).

Methods

The participants were 7 obligate carriers of protanomaly (cPa), 24 obligate carriers of deuteranomaly (cDa), 12 female controls (fCo), and 10 male controls (mCo). The average ages of the four groups were 52.7 (41–66), 52.3 (38–68), 47.3 (38–76), and 47.7 (37–65) years, respectively. The means did not differ significantly ($F(3, 49) = 1.4, p = 0.25$). In the case of carriers, we tested at least one anomalous offspring, usually sons but in the case of one carrier, three deuteranomalous daughters. Initially, color-deficient children were recruited either as a result of a television feature about the research or through a local school. The mothers of selected cases were invited to take part in the study. Control participants were recruited through the university staff network or were friends of the mothers. Ethical permission was given by the research committee of the North East Strategic Health Authority (ref 04/Q0905/62). Genetic analysis on the DNA of the participants was approved by the institutional review board: Human Subjects Committee of the University of Washington.

Rayleigh match mid-points and matching ranges were established using the Oculus anomaloscope (Optikgeräte GmbH, Wetzlar). For a range of red/green ratios set by the examiner, participants were asked to equate the brightness of the mixture and monochromatic fields and were then asked whether the fields matched in hue. For each ratio, the participants rated the quality of the match on a 5-point scale, where 5 indicated a perfect match. Only ratios scoring 5 were used to derive the matching range. Participants used their preferred eye.

Results and discussion

In Figure 2, we show Rayleigh match mid-points and matching ranges for deutan and protan carriers, for their color-deficient offspring, and for the male and female controls. The carriers and the controls are ordered, within each group, according to their match mid-points. Related offspring are shown against each carrier. Colored symbols identify participants who took part in the multidimensional scaling test described below. The red symbols represent those participants who had more than one dimension on the test, whereas those with blue symbols had only one dimension on the test. For details, see below.

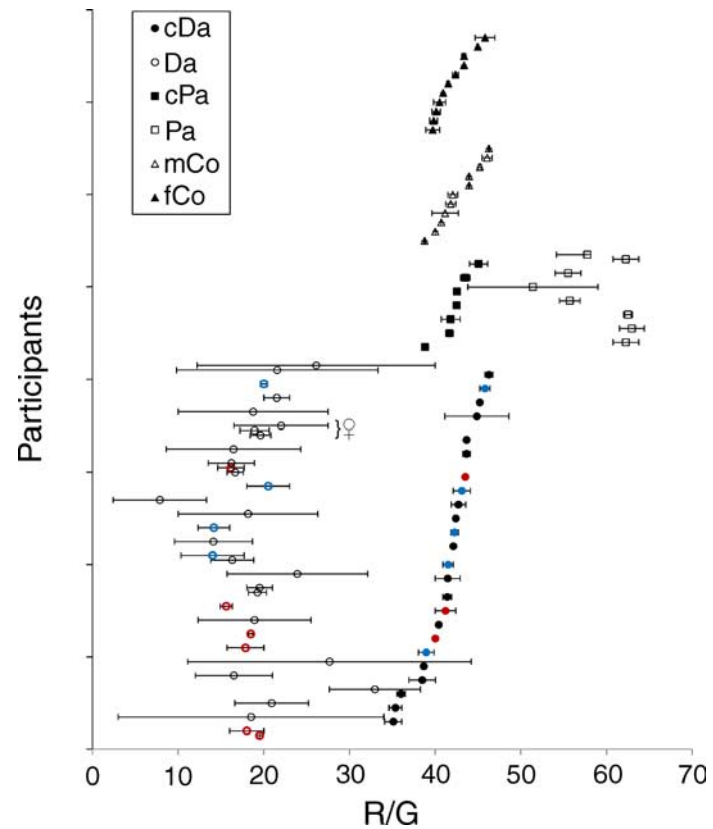


Figure 2. Rayleigh match-midpoints and ranges for all carriers and their color-deficient offspring as well as female and male control participants. For explanation see text.

From the data of Figure 2, several interesting points arise:

1. For both match mid-points and ranges, one-way analyses of variance were performed for the four groups: male and female controls and protan and deutan carriers. There were no significant differences between groups for either mid-points ($F(3, 48) = 0.51, p = 0.67$) or matching ranges ($F(3, 48) = 1.01, p = 0.39$). However, there were a few deutan carriers with unusually low match mid-points, an observation similar to that made by Waaler (1927).
2. There was no significant correlation between the match mid-points of protan carriers and those of their sons ($r = -0.15, p = 0.73$) nor between the mid-points of deutan carriers and those of their sons ($r = -0.28, p = 0.18$).
3. Similarly, there were no significant correlations between the matching ranges of carriers and their sons (for protans $r = -0.59, p = 0.15$; for deutans $r = 0.18, p = 0.39$).
4. One carrier of deuteranomaly (cDa29) did not accept any match on the Oculus anomaloscope. Her sons' matches are shown at the very bottom of Figure 2.

5. Within the group of deuteranomalous offspring, there was a small but significant correlation between match mid-points and matching ranges ($r = 0.37$, $p = 0.034$).

Rayleigh discriminations

It is provocative when carriers of color anomalies refuse Rayleigh matches as in the case of cDa29 in the present study and in the case of eight carriers of anomaly in the large-field Rayleigh match study of Jordan and Mollon (1993). However, the conventional Rayleigh match is a criterion-dependent task, and the dimensionality of color vision is more securely established by a forced-choice discrimination task than by subjective matching (Cornsweet, 1970): Rather than asking whether two stimuli look alike, one ought to establish whether the potential tetrachromat can objectively discriminate them.

In the present test, the task was a three-alternative, temporal forced choice, essentially a performance version of the Rayleigh match. On each trial, two of the three presentations were of a monochromatic orange light and the third was of a mixture of a red and a green light; the participant was asked to indicate the odd one out. Across trials, the computer sampled the space defined by (a) the red/green ratio and (b) the luminance of the monochromatic field. Within this space, first explicitly defined by Franceschetti (1928), the normal observer is dichromatic since the S cones are very insensitive.

Methods

Participants were 18 deutan and 7 protan carriers, 10 male and 12 female controls. All had participated in the preceding measurements of Rayleigh matches.

Discrimination of light stimuli in the Franceschetti space was measured using a purpose-built Maxwellian-view colorimeter. Light from a single tungsten-halogen source was drawn by custom-made fiber-optic light guides to the inputs of three monochromators (Jobin-Yvon Triax 180). Each fiber bundle was formed into a linear array and was imaged onto the input slit of its respective monochromator. This optical coupling minimized stray light and maximized throughput. The full bandwidths of the monochromators were set to be 3.5 nm at half height. The output of each monochromator was collimated and refocused on a high-speed shutter (Uniblitz). Placed close to this focus was a neutral-density wedge (1 log unit), mounted on a servo motor. All three beams were combined with cube beam splitters and then refocused on a piece of ground glass mounted on a 2-mm aperture. The latter served as a secondary source, and it was this source, relayed by two

lenses, that was focused on the participant's pupil. A single circular field stop in this final common channel defined the 2-deg disc seen by the participant.

In order to minimize any cues arising from chromatic aberration at the edges of the mixture field, an ancillary CRT monitor was used to display a mask of dynamic luminance and chromatic noise. An image of the monitor screen was formed in the same plane as the field stop that defined the primary stimulus disc. Thus, the participant saw the annular mask superposed on the edges of the stimulus. To prevent the participant using auditory cues from the shutters, he or she wore headphones over which white noise was played.

On each trial, three stimuli were presented in rapid succession, two of them being a monochromatic orange light (590 nm) and the third a mixture of a red (670 nm) and a green (546 nm) light (see Figure 3A). Each stimulus field was presented for 150 ms and the inter-stimulus interval was 300 ms. The luminances of the red and green primaries were equal (60 td). The position of the mixture field in the trial sequence was randomized, and the participant was asked to indicate its position by pushbuttons.

In random order, the computer sampled a two-dimensional stimulus grid of 90 cells defined by (a) 10 ratios of the 670- and 546-nm components of the mixture field and (b) 9 luminances of the monochromatic 590-nm field. In an initial practice run, only stimuli from the outer corners of this sampling space were used. A further practice block of 90 trials gave participants experience of the entire stimulus array, each trial sampling a different combination of red-green ratio and luminance of the monochromatic standard. Thereafter, there were three experimental blocks of 90 trials each; thus, three independent estimates were made of accuracy and speed for each cell.

For a normal trichromat, we expected there to be a combination of the red/green ratio ($R_{670} / (R_{670} + G_{546})$) and of the luminance of the monochromatic orange field (I_{590}) at which the participant would fail to discriminate and would exhibit long response times. These values of ($R_{670} / (R_{670} + G_{546})$) and I_{590} would correspond to the classical Rayleigh match but are based on performance rather than on subjective judgment. In contrast, a tetrachromat should be able to discriminate at all combinations of ($R_{670} / (R_{670} + G_{546})$) and I_{590} .

Results and discussion

Since we could not assume a particular Rayleigh match in advance, our algorithm searched, in random sequence, a matrix of combinations of ($R_{670} / (R_{670} + G_{546})$) and I_{590} that enclosed the full range of possibilities. The upper panel of Figure 3B shows, for a typical male control, the distribution of response times within this matrix, and the lower panel shows the distribution of errors. It can be seen that the region of stimulus combinations that yields errors

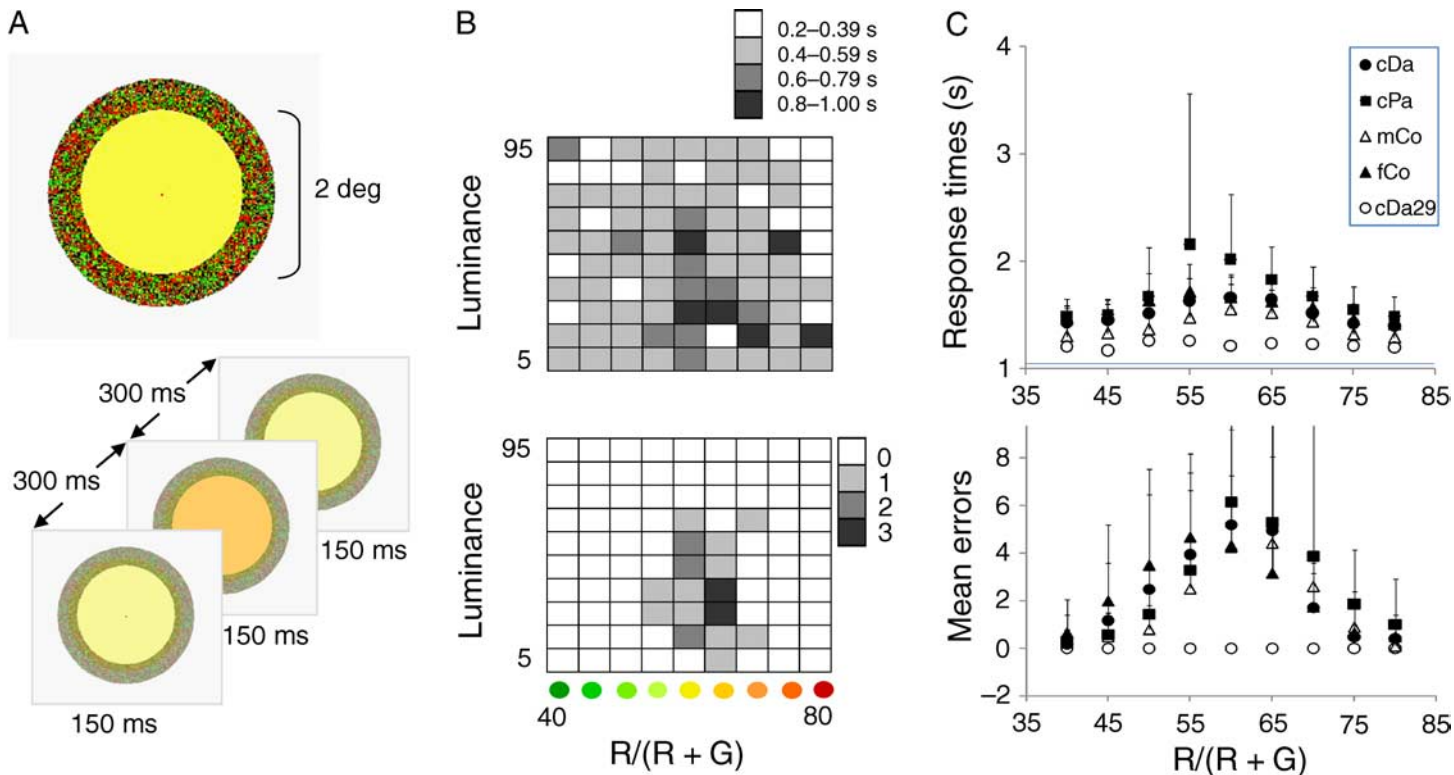


Figure 3. Rayleigh discrimination test. (A) Spatial arrangement of stimulus field (upper panel) and sequence of stimuli in one trial. Superposed on the edge of the field was an annulus of dynamic spatio-chromatic noise, which served to mask any chromatic aberration that could provide an additional cue to the discrimination. The duration of each stimulus field was 150 ms. The dark inter-stimulus interval was 300 ms. The participant's task was to identify which of the three successive fields was a red-green mixture. (B) Distribution of response times (upper panel) and errors (lower panel) in the I_{590} , ($R_{670} / (R_{670} + G_{546})$), matrix for one typical normal male observer. The red/green ratios are expressed as percentage of luminance contributed by the 670-nm primary in the red/green mixture. (C) Mean response times (upper panel) and number of errors (lower panel) for different participant groups as a function of the red-green ratio of the mixed field. Filled circles, 17 carriers of deuteranomaly (cDa); filled squares, 7 carriers of protanomaly (cPa); open triangles, 10 male controls (mCo); filled triangles, 12 female controls (fCo). Error bars denote +1 standard deviation of the means. Response times were measured from the onset of the first of the three stimuli. The horizontal, dotted line corresponds to the offset of the third stimulus field. The open circles represent a single carrier of deuteranomaly, cDa29, who exhibits the fastest response times with no clear peak, and makes no errors at any ratio. Her data are not included in the cDa group.

is also a region of long response times. Figure 3C summarizes the performance of two carrier groups and two normal control groups. Response times (upper panel) and error rates (lower panel), averaged across different values of I_{590} , are shown as a function of ($R_{670} / (R_{670} + G_{546})$). All groups exhibit a maximum at an intermediate value of ($R_{670} / (R_{670} + G_{546})$), and the positions of the peaks are similar for the two independent performance measures. An ANOVA revealed that there is no difference between groups in the means of errors made for different positions of $R / (R + G)$ ($F(3, 43) = 1.67, p > 0.19$). Some of the response times differ significantly between groups, but this difference is not restricted to any specific region of our grid and we therefore conclude that it is caused by individual differences in response times unrelated to color vision.

However, one participant cDa29 (represented by open circles) behaves as if she has access to an additional cone signal: she made no errors at any value of ($R_{670} / (R_{670} +$

$G_{546})$) (see Figure 3C, lower panel) and her response times not only are faster than those of other participants ($M = 1.221$ s from onset of first stimulus) but are roughly even across the stimulus space (see Figure 3C, upper panel). The same accuracy and similar response times were obtained on a retest after two months. This participant has two deuteranomalous sons and one normal son and thus is necessarily heterozygous. Recall that this carrier did not accept any match on the Oculus anomaloscope. She read the Ishihara plates without error.

Perhaps the most important result of our Rayleigh discrimination test is that most carriers exhibit a region of the Franceschetti space in which their discrimination is impaired in the same way as is found for color-normal controls. Thus, by this test, the great majority of carriers show no sign of tetrachromacy.

cDa29 is the single exception. If we accept for the moment that she is behaviorally tetrachromatic, her behavioral

tetrachromacy could arise in one of two ways. Firstly, she might enjoy “strong tetrachromacy”: in any one small region of her visual field, she may have access to both normal and deuteranomalous color signals, and her color space may be truly four-dimensional. Secondly, her retina may be a relatively coarse mosaic of normal and deuteranomalous patches, and in any one patch she may not have concurrent access to both the normal and the deuteranomalous signals. In this case, when presented with red-green ratios near the normal match, she might rely on signals from the deuteranomalous patches in her retina; and when presented with ratios near the deuteranomalous match, she might rely on signals from normal patches. Subjectively, the stimulus fields might appear blotchy to the observer. We did ask cDa29 whether the 2-deg field appeared patchy to her. Her response was negative.

However, we have to ask whether other factors could have contributed to cDa29’s flawless discrimination performance on the Rayleigh test. (1) We discount the effects of chromatic aberrations, as we took great care to mask any possible cues at the edges of the mixture field. The experimenter spent some time at the beginning of each session to help align the participants’ eyes in Maxwellian view. No participant reported residual edge effects. (2) We cannot entirely exclude detection by either S-cones or rod signals, but their effects must be negligible since S-cone sensitivity is minimal at 546 nm, and the luminance of the stimuli was within the photopic range. If there had been any significant stimulation of these other two receptor systems, then these signals should have been available to other carriers and normal controls as well. (3) A final possibility is that cDa29, unlike other observers, is able to exploit the spatial gradient in the density of macular pigment across the central fovea, but absorption by the macular pigment is in fact negligible at the wavelength of our shortest (546 nm) primary (Bone, Landrum, & Cairns, 1992).

Dimensionality of color space measured by multidimensional scaling

Our second test used multidimensional scaling (MDS) (Kruskal, 1964; Shepard, 1962) to reveal the extra dimension of a tetrachromat’s color space. The input to an MDS program is a matrix of judged similarities of all possible pairs of a set of stimuli; its output is a map of these stimuli that minimizes the differences between the input proximities and the corresponding proximities in the derived space.

We used an MDS test that we have specifically designed to reveal a deuteranomalous dimension of color space: the test contains pairs of stimuli that are near

metameric for the normal observer but are calculated to be distinct for the deuteranomalous (Bosten, Robinson, Jordan, & Mollon, 2005).

For this test, we selected a subset of our deuteranomalous carriers on the basis of the anomaloscope matching ranges of their sons. We reasoned that tetrachromacy was most likely to be manifest in those carriers whose sons have a small matching range and thus may have a large spectral separation between their L and L’ pigments (Regan et al., 1994).

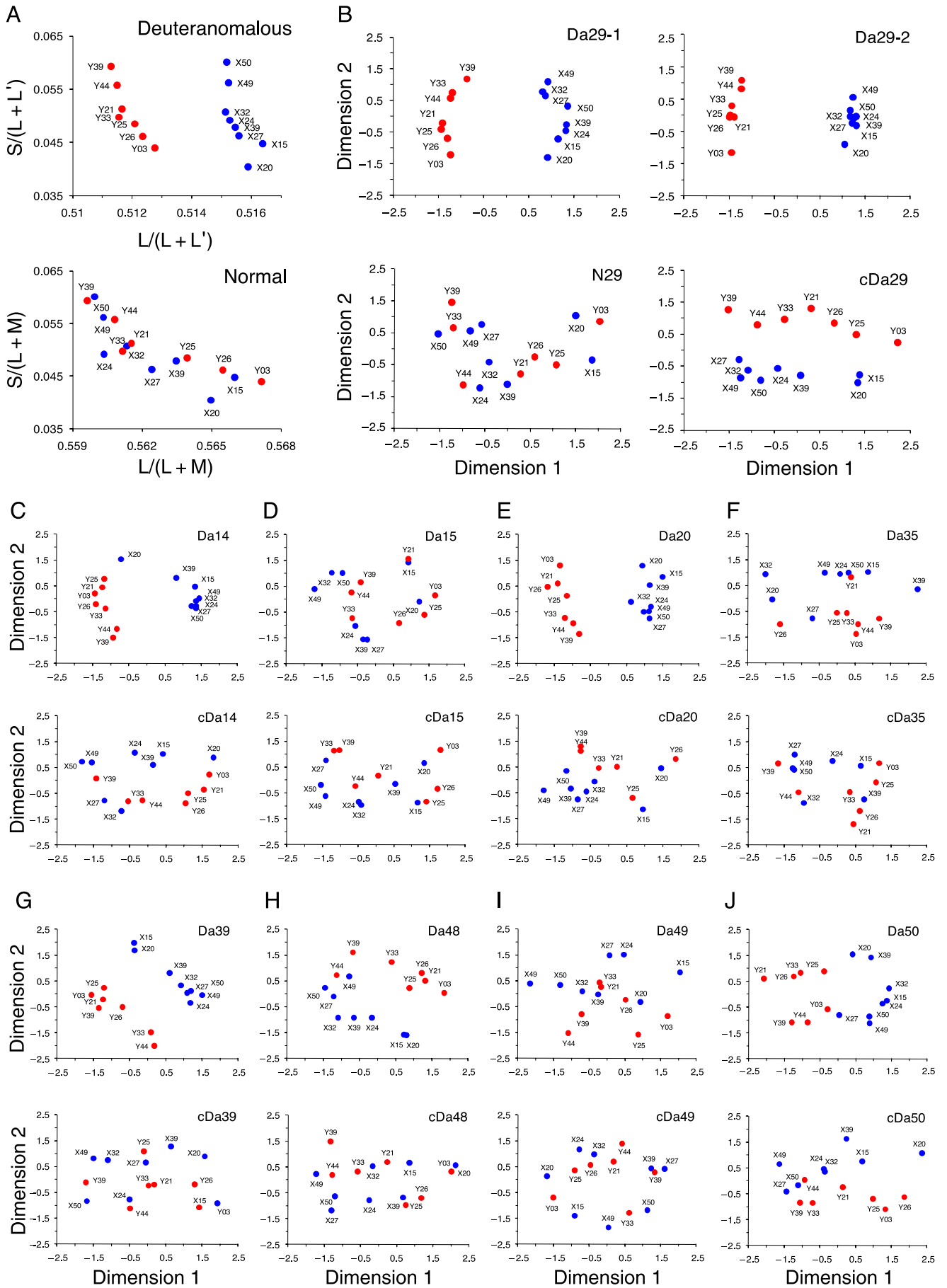
Methods

Participants were 9 carriers of deuteranomaly, 10 of their male, deuteranomalous sons and one normal son. These participants are identified by colored symbols in Figure 2. We chose deuteranomalous carriers whose anomalous sons had matching ranges on the Oculus anomaloscope extending from 0 (in the case of one son of cDa29) to 4.3 Nagel units. We also tested 6 female and 10 male controls, some of whom were newly recruited for this test. No protan carriers were tested since the MDS test was designed to detect the unique deuteranomalous dimension.

Stimuli were 15 colored discs subtending 4.5° at a typical viewing distance. Two stimulus sets were used: one painted with mixtures of cobalt blue and cadmium yellow single-pigment acrylics (X) and one painted with mixtures of yellow oxide and ultramarine blue (Y).

In selecting suitable subsets of X and Y discs, we modeled the photon catches of individual cone types when exposed to light from a given stimulus under the experimental illuminant (a broadband amber). Using a spectroradiometer (PhotoResearch 650) at the position of the observer’s eye, we measured the spectral power distribution of each disc ($E(\lambda)$) and multiplied it in turn by the spectral sensitivities of S, M, L, and anomalous (L’) cones ($\varphi_{(S)}(\lambda)$, $\varphi_{(M)}(\lambda)$, $\varphi_{(L)}(\lambda)$, and $\varphi_{(L')}(\lambda)$). We used cone sensitivities as estimated by DeMarco et al. (1992) and Smith and Pokorny (1975). We normalized all the cone sensitivities since it is not known how the scaling of the anomalous photopigment relates to that of the normal. Integrating each product between 400 and 700 nm gave the photon catches in the four classes of cone. The chromatic signals available to a normal and to a deuteranomalous observer could then be modeled as ratios of cone activations, e.g., $(\int \varphi_{(M)}(\lambda) \cdot E(\lambda) \delta\lambda) / (\int \varphi_{(L)}(\lambda) \cdot E(\lambda) \delta\lambda)$. Further information on this test can be found in Bosten et al. (2005).

Importantly, we included pairs of samples with spectral power distributions that we had calculated to be distinguishable to a hypothetical deuteranomalous observer (DeMarco et al., 1992), but to be indistinguishable metamers for a normal. We plotted the positions of our stimuli in a color space similar to that of MacLeod and Boynton (1979), but where the cone sensitivities are



normalized. The X and Y subsets of stimuli fall along a single line in this color space (see [Figure 4A](#), lower panel), but they are separated in an analogous space constructed for the hypothetical deuteranomalous observer (see [Figure 4A](#), upper panel). We have previously shown that, in practice, the X and Y stimulus subsets are readily separated by many deuteranomalous participants but not by normals (Bosten et al., 2005). We here ask whether carriers of deuteranomaly can make the discriminations made by their anomalous sons.

Participants rated the dissimilarity of all possible pairs of stimulus discs on a scale from 0 to 10. Non-metric MDS was used to reconstruct a subjective space from the matrix of dissimilarity judgments for each observer. We used non-metric, rather than metric, MDS since it is safest to treat the dissimilarity ratings as an ordinal scale: the verbal ratings given by the participants cannot be assumed to be linearly related to the internal signal on which they are based (Kruskal, 1964).

Results and discussion

Panel A of [Figure 4](#) shows the theoretical MDS solutions expected for a deuteranomalous observer (top) and for a normal observer (bottom). The deuteranomalous observer is assumed to rely on the chromatic dimensions $S / (L + L')$ and $L / (L + L')$. The modeled data show a clear separation between the X and Y pairs described in [Methods](#) above. The normal observer is assumed to rely on the chromatic dimensions $S / (L + M)$ and $L / (L + M)$, and in the modeled data the X and Y subsets fall on a single line.

Figure 4. Multidimensional scaling experiment. (A) Chromaticities of 15 colored discs modeled in a color space for a standard normal observer (lower panel) and an analogous space for a hypothetical deuteranomalous observer (upper panel). The X (blue circles) and Y (red circles) stimulus subsets are separated on the deuteranomalous dimension $L / (L + L')$ but form a single array and are intermingled on the normal dimensions $L / (L + M)$ and $S / (L + M)$. (They are also intermingled on the normal and deuteranomalous luminance dimensions $L + M$ and $L + L'$.) (B) Multidimensional scaling solutions for the two deuteranomalous sons of cDa29 (top), for her normal son (bottom left) and for cDa29 herself (bottom right). Her normal son does not separate the two subsets of stimuli that are clearly separated by his deuteranomalous brothers. His solution is horseshoe shaped and his data might be adequately described by a one-dimensional solution (Rodieck, 1977). cDa29 separates the X and Y subsets, but the second dimension of her solution corresponds to the first dimension of the solutions for her deuteranomalous sons, thus leading to a rotation of her space. (C–J) MDS solutions for all other heterozygous mother and son pairs tested. Results for deuteranomalous sons are always represented in the upper panel. Correlations with color dimensions are given in [Table 1](#).

In discussing the experimental results from the separate groups of participants, we take as a quantitative measure the Spearman rank correlation between the empirical ordering of the chips and their ordering on the modeled dimensions. We give below the correlations and significance values without correction for multiple correlations: a more conservative estimate would mean that fewer carriers would show a two-dimensional solution.

Of the 16 control subjects (6 female, 10 male), none gave a two-dimensional solution. Fourteen gave a one-dimensional solution that correlated with $S / (L + M)$ ($n = 13$, $0.632 \leq r_s \leq 0.857$, $p < 0.011$) or $L / (L + M)$ ($n = 1$, $r_s = 0.679$, $p = 0.005$) and 2 gave a 0-dimensional solution where no dimensions correlated with any dimension modeled and were assumed to represent noise.

Of the 10 deuteranomalous sons tested, 6 gave two-dimensional solutions (see [Figure 4](#), upper panels of B, C, E, G and J) where one dimension correlated with $L / (L + L')$ ($n = 6$, $0.579 \leq r_s \leq 0.882$, $p < 0.016$) and the other with $S / (L + L')$ ($n = 6$, $0.604 \leq r_s \leq 0.850$, $p < 0.017$) and 4 gave one-dimensional solutions that correlated with $S / (L + L')$ ($n = 2$, $0.782 \leq r_s \leq 0.918$, $p < 0.001$) or $L / (L + L')$ ($n = 2$, $0.621 \leq r_s \leq 0.775$, $p < 0.013$). The sons who gave two-dimensional solutions are identified in [Figure 2](#) by the red symbols.

Of the nine carriers of deuteranomaly tested, four gave two-dimensional solutions (see [Figure 4](#), lower panels of B, C, E and J), where the first axis correlated with $S / (L + M)$ ($n = 4$, $0.714 \leq r_s \leq 0.807$, $p < 0.001$) and where the second correlated with $L / (L + L')$ ($n = 4$, $0.643 \leq r_s \leq 0.825$, $p < 0.01$). The remainder gave one-dimensional solutions that correlated with $S / (L + M)$ ($n = 5$, $0.696 \leq r_s \leq 0.889$, $p < 0.004$). Correlations for individual carriers are shown in [Table 1](#).

In [Figure 4B](#) (upper panels), we show the MDS solutions for the two deuteranomalous sons of participant cDa29. Both solutions are clearly two-dimensional and resemble closely the theoretical deuteranomalous space (see [Figure 4A](#), upper panel). The first dimension correlates with the theoretical anomalous signal $L / (L + L')$ [Da29-1: $r_s = 0.711$, $p = 0.003$; Da29-2: $r_s = 0.729$, $p = 0.002$], whereas their second dimension correlates with $S / (L + L')$ [Da29-1: $r_s = 0.85$, $p < 0.001$; Da29-2: $r_s = 0.825$, $p < 0.001$]. The lower left panel of [Figure 4B](#) shows the MDS solution for cDa29's normal son, N29. As expected, he does not separate the X and Y subsets. His first dimension correlates with the two normal ratios $S / (L + M)$ [$r_s = 0.818$, $p < 0.001$] and $L / (L + M)$ [$r_s = 0.911$, $p < 0.001$], but his second dimension does not correlate significantly with $L / (L + L')$ [$r_s = 0.07$, $p = 0.79$] or with any other modeled dimension and probably represents only noise.

Of special interest is the MDS solution for the mother, cDa29 (see [Figure 4B](#), lower right panel). Although her solution is rotated relative to those of her anomalous sons, she clearly separates the X and Y stimulus subsets. Her first dimension correlates, as expected, with the cone ratios of the color normal space $S / (L + M)$ [$r_s = 0.807$,

ID		cDa14	cDa15	cDa20	cDa29	cDa35	cDa39	cDa48	cDa49	cDa50	
Mother's Genotype	M	M(ala ¹⁸⁰)	M(ala ¹⁸⁰)	M(ala ¹⁸⁰)	M(ala ¹⁸⁰)	-	M(ala ¹⁸⁰)	M(ala ¹⁸⁰)	-	M(ala ¹⁸⁰)	
	L'	M3L4	M4L5	M2L3(ser ¹⁸⁰)	M4L5	-	M3L4	M3L	-	M4L5	
	L1	L(ser ¹⁸⁰)	L(ser ¹⁸⁰)	L(ser ¹⁸⁰)	L(ser ¹⁸⁰)	-	L(ala ¹⁸⁰)	L(ala ¹⁸⁰)	-	L(ser ¹⁸⁰)	
	L2	L(ser ¹⁸⁰)	L(ser ¹⁸⁰)	L(ser ¹⁸⁰)	L(ser ¹⁸⁰)	-	L(ser ¹⁸⁰)	L(ser ¹⁸⁰)	-	L(ser ¹⁸⁰)	
Peak sensitivity (nm) from Merbs & Nathans (1992a)	M	529.7	529.7	529.7	529.7	-	529.7	529.7	-	529.7	
	L'	548.8	544.8	553	544.8	-	548.8	548.8	-	544.8	
	L1	556.7	556.7	556.7	556.7	-	552.4	552.4	-	556.7	
	L2	556.7	556.7	556.7	556.7	-	556.7	556.7	-	556.7	
L'-L separation (nm)		7.9	11.9	3.7	11.9	-	7.9	7.9	-	11.9	
Peak sensitivity (nm) from Asenjo et al. (1994)	M	532	532	532	532	-	532	532	-	532	
	L'	555	551	559	551	-	555	555	-	551	
	L1	563	563	563	563	-	556	556	-	563	
	L2	563	563	563	563	-	563	563	-	563	
L'-L separation (nm)		8	12	4	12	-	8	8	-	12	
Oculus Anomaloscope (sons)	mid-point	15.6	14.1	16.15	1) 19.2; 2) 18	20	17.85	20.5	16.3	18.45	
	range	1.4	3.7	3.1	1) 0; 2) 4	0.8	4.3	5	5	0.45	
Oculus Anomaloscope (mothers)	mid-point	41.2	42.25	43.5	-	45.8	38.95	43.1	41.5	40	
	range	2.4	0.9	0	-	1.2	1.8	2	1.2	0	
MDS (sons)	S/(L+L')	r _s	0.607	0.782	0.732	1) 0.850; 2) 0.825	-	-	0.603	0.917	0.65
		p	0.016**	<0.001**	0.002**	1) <0.001**; 2) <0.001**	-	-	0.017**	<0.001**	0.009
	L'/(L+L')	r _s	0.579	-	0.782	1) 0.711; 2) 0.729	0.621	0.775	0.882	-	0.8
		p	0.023	-	<0.001**	1) 0.003**; 2) 0.002**	0.013**	<0.001**	<0.001**	-	<0.001**
	Dimension		2	1	2	1) 2; 2) 2	-	-	1	1	2
	Dimension		1	-	1	1) 1; 2) 1	1	1	2	-	1
MDS (mothers)	S/(L+M)	r _s	0.761	0.771	0.714	0.807	0.889	0.786	0.85	0.696	0.807
		p	0.001**	<0.001**	0.003**	<0.001**	<0.001**	<0.001**	<0.001**	0.004**	<0.001**
		Dimension	1	1	1	1	1	1	1	1	1
	L/(L+M)	r _s	0.861	0.911	0.814	0.932	0.939	0.814	0.936	0.786	0.907
		p	<0.001**	<0.001**	<0.001**	<0.001**	<0.001**	<0.001**	<0.001**	<0.001**	<0.001**
		Dimension	1	1	1	1	1	1	1	1	1
L'/(L+L')	r _s	0.65	0.35	0.64	0.82	0.47	0.18	0.2	0.21	0.71	
	p	0.009**	0.2	0.01**	<0.001**	0.08	0.49	0.47	0.44	0.003**	
	Dimension	2	-	2	2	-	-	-	-	2	

Table 1. Data for nine carriers of deuteranomaly and their sons. The first three horizontal sections show the carriers' genotypes and corresponding peak sensitivities according to both Asenjo et al. (1994) and Merbs and Nathans (1992a). Also shown are the anomaloscope mid-points and matching ranges for both sons and mothers and their respective color dimensions on the MDS test. The DNA for cDa35 and cDa49 degraded before analyses and therefore data are unavailable.

$p < 0.001$] and L / (L + M) [$r_s = 0.932$, $p < 0.001$]. However, her second dimension correlates with the first dimension of her anomalous sons [Da29-1: $r_s = 0.771$, $p < 0.001$; Da29-2: $r_s = 0.65$, $p = 0.009$] and also with the theoretical deuteranomalous dimension L / (L + L') [$r_s = 0.825$, $p < 0.001$]. Thus, this heterozygote is capable both

of the discriminations made by her anomalous sons and of those made by her normal son.

How unusual is cDa29's ability to discriminate along the "anomalous" axis? Recall that none of 16 control participants separated the X and Y stimulus subsets or exhibited a dimension that correlated significantly with L / (L + L').

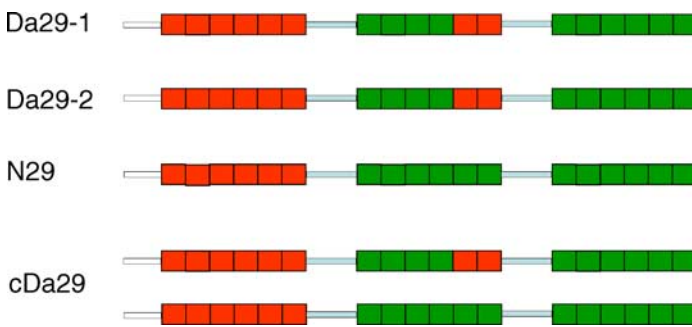


Figure 5. Opsin gene arrays in the candidate tetrachromat cDa29 and her three sons. The two deuteranomalous sons (Da29-1 and Da29-2) exhibit a long-wave gene that encodes an opsin with normal peak sensitivity (but see text for further discussion) and a hybrid gene in which exons 1–4 correspond to the M sequence and exons 5–6 correspond to the L sequence. The third, middle-wave gene in the array is thought not to be expressed. For inferred peak sensitivities of the corresponding photopigments, please see Table 1.

Besides cDa29, three further carriers (cDa14, cDa20, and cDa50; all with sons who did exhibit two-dimensional MDS solutions) had a dimension—always the second one in the two-dimensional MDS solution—that correlated significantly with the theoretical anomalous axis [$0.643 \leq r_s \leq 0.711$, $p < 0.01$]. However, these carriers differed from cDa29 in that they exhibited a localized region of errors on our Rayleigh discrimination test.

Molecular genetic analysis

Saliva samples were obtained from all carriers and their male offspring, and the X chromosome opsin arrays were sequenced.

Methods

DNA from saliva samples was prepared using the OraGene DNA Purification Kit and protocol. Analysis of the sequence of opsin genes was performed according to the procedure described by Oda, Ueyama, Nishida, Tanabe, and Yamade (2003). Briefly, the first genes and the downstream genes were independently amplified by long-range polymerase chain reaction (PCR). The PCR products were used as templates to separately amplify the exons. The secondary PCR products were sequenced directly by Dye Terminator Cycle Sequencing Kit and a PRISM 310 Genetic Analyzer (Applied Biosystems, Foster City CA, USA). The primers and conditions used to amplify the exons are given by Deeb, Hayashi, Windericks, and Yamaguchi (2000).

Results

In Table 1, all nine carriers who participated in the MDS test are listed. The first section shows their genotypes, the second and third sections show the inferred λ_{\max} values of their M, L' , and two L-cone photopigment variants. Two sets of values are given: one is taken from Merbs and Nathans (1992a) the other from Asenjo, Rim, and Oprian (1994). For a discussion on the use of the two sets, please see the Appendix A. Also shown in the table are the mid-points and ranges on the anomaloscope for sons and mothers as well as their performance on the MDS test. The inferred separation of the two pigments of the deutan sons ranges from 12 nm to as little as 4 nm, even though all these sons were selected for having restricted matching ranges on the anomaloscope.

Figure 5 shows the inferred gene arrays of cDa29 and her three sons. The opsin arrays of her normal (N29) and anomalous sons (Da29-1 and Da29-2) suggest that she herself has a hybrid gene in which exons 1–4 exhibit the normal M sequence and exons 5–6 exhibit the normal L sequence and that, in addition to this hybrid gene, she has normal L and M pigment genes. These inferences from her sons' X chromosomes were confirmed by direct sequencing of her own DNA.

Table 2 shows the full amino acid sequences for the first and second genes of cDa29's normal and deuteranomalous sons. We note one curiosity in the sequence of the first gene of the deuteranomalous sons: the sequence is that of a wild-type long-wave gene (Nathans et al., 1986) except that at site 153, leucine is replaced by methionine. The latter is characteristic of the wild-type middle-wave sequence, but it is not thought to affect the λ_{\max} of the photopigment (Asenjo et al., 1994).

General discussion

Carriers of deuteranomaly constitute about 10% of all women (Pokorny, Smith, Verriest, & Pinckers, 1979), but most carriers in our sample showed little evidence of a salient tetrachromatic signal. Our one candidate for strong tetrachromacy is cDa29. Is there one and only one critical factor determining her phenotype? One important factor ought to be the spectral separation of her photopigments. Her hybrid (L') gene draws exons 1–4 from the normal M sequence and exons 5–6 from the normal L sequence (see Figure 5 and Table 2). In addition, she has normal M and L genes. From the *in vitro* experiments of Merbs and Nathans (1992a), we should expect the corresponding M, L' , and L photopigments to peak at approximately 530, 545, and 557 nm, giving a large spectral separation of 12 nm between L' and L. (The alternative *in vitro* estimates of Asenjo et al. (1994) give different λ_{\max} values of 532, 551 and 563 nm for the M, L' and L photopigments, but a

N29

FIRST GENE (L)

EXON 2 (L)

gcccttcgaaggcccgaattaccacatcgctcccagatgggtgtaccacctcaccagtgct
 P F E G P N Y H I A P R W V Y H L T S V
 tggatgatctttgtggctactgcacccgtcttcacaaatgggcttgtgctggcggccacc
 W M I F V V **T** A S V F T N G L V L A A T
 atgaagttcaagaagctgcgccacccgctgaactggatcctggatgaacctggcggctcgt
 M K F K K L R H P L N W I L V N L A V A
 gacctagcagagaccgtcatcgccagcactatcagcattgtgaaccagggtctctggctac
 D L A E T V I A S T I S I V N Q V **S** G Y
 ttcgtgctgggcccaccctatgtgtgtcctggagggtacaccgtctccctgtgtg
 F V L G H P M C V L E G Y T V S L C

EXON 3 (L)

ggatcacagggtctctgggtctctggccatcatttcctgggagaggtggctgggtgggtgtgcaag
 I T G L W S L A I I S W E R W L V V C K
 ccctttggcaatgtgagatttgatgccaaagctggccatcgtgggcattgccttctcctgg
 P F G N V R F D A K L A I V G I A F S W
 atctgggtctgctgtgtggacagccccgccatctttggttgagcag
 I W **S** A V W T A P P I F G W S

Exon 4 (L)

gtactggccccacggcctgaagacttcatgcggcccagacgtgttcagcggcagctcgtac
 Y W P H G L K T S C G P D V F S G S S Y
 cccggggtgcagctcttacatgattgtcctcatggtcacctgctgcatcatccactcgtc
 P G V Q S Y M I V L M V T C C I **I** P L **A**
 atcatcatgctctgctacctccaagtgtggctggccatccgagcg
 I I M L C Y L Q V W L A I R A

EXON 5 (L)

gtggcaaagcagcagaaagagtctgaatccaccagaaggcagagaaggaagtgacgcgc
 V A K Q Q K E S E S T Q K A E K E V T R
 atgggtgggtgatgatctttgcgtactgcgtctgctggggaccctacaccttcttcgca
 M V V V M I F A **Y** C V C W G P Y **T** F F A
 tgctttgctgctgccaacctggttacgccttccaccctttgatggctgccctgcccggcc
 C F A A A N P G Y A F H P L M A A L P A
 tactttgccaaaagtgccactatctacaacccgttatctatgtctttatgaaccggcag
 Y F A K S A T I Y N P V I Y V F M N R Q

Second Gene (M)

Exon 2 (M)

gcccttcgaaggcccgaattaccacatcgctcccagatgggtgtaccacctcaccagtgtc
 P F E G P N Y H I A P R W V Y H L T S V
 tggatgatctttgtgggtcattgcatccgtcttcacaaatgggcttgtgctggcggccacc
 W M I F V V **I** A S V F T N G L V L A A T
 atgaagttcaagaagctgcgccaccgctgaactggatcctggtgaacctggcgggtcgct
 M K F K K L R H P L N W I L V N L A V A
 gacctggcagagaccgtcatcgccagcactatcagcgttgtgaaccaggtctatggctac
 D L A E T V I A S T I S V V N Q V **Y** G Y
 ttcgtgctgggcccaccctatgtgtgtcctggagggtacaccgtctccctgtgtg
 F V L G H P M C V L E G Y T V S L C

Exon 3 (M)

ggatcacaggctctctgggtctctggccatcatttctctgggagagatggatgggtgggtctgcaag
 I T G L W S L A I I S W E R W M V V C K
 cccttggcaatgtgagatttgatgccaaagctggccatcgtgggcattgccttctcctgg
 P F G N V R F D A K L A I V G I A F S W
 atctgggctgctgtgtggacagccccgccatctttggttgagcag
 I W **A** A V W T A P P I F G W S

Exon 4 (M)

gtactggccccacggcctgaagacttcatgcgccagacgtgttcagcggcagctcgtac
 Y W P H G L K T S C G P D V F S G S S Y
 cccggggtgcagtcttacatgattgtcctcatggtcacctgctgcatcaccactcagc
 P G V Q S Y M I V L M V T C C I **T** P L **S**
 atcatcgtgctctgctacctccaagtgtggctggccatccgagcg
 I I V L C Y L Q V W L A I R A

EXON 5 (M)

gtggcaaagcagcagaaagagtctgaatccaccagaaggcagagaaggaagtgacgcgc
 V A K Q Q K E S E S T Q K A E K E V T R
 atgggtgggtgatgggtcctggcattctgcttctgctggggaccctacgccttcttcgca
 M V V V M V L A **F** C F C W G P Y **A** F F A
 tgctttgctgctgccaacctggctacccttccaccctttgatggctgacctgcccggcc
 C F A A A N P G Y P F H P L M A A L P A
 ttctttgccaaaagtgcactatctacaacccggttatctatgtctttatgaaccggcag
 F F A K S A T I Y N P V I Y V F M N R Q

DA29-1 and DA29-2

FIRST GENE (L)

EXON 2 (L)

gcccttcgaaggcccgaattaccacatcgctcccagatgggtgttaccacctcaccagtgtc
 P F E G P N Y H I A P R W C Y H L T S V
 tggatgatctttgtggctactgcacccgtcttcacaaatgggcttgtgctggcggccacc
 W M I F V V T A S V F T N G L V L A A T
 atgaagttcaagaagctgcgccacccgctgaactggatcctggatgaacctggcggctcgt
 M K F K K L R H P L N W I L V N L A V A
 gacctagcagagaccgtcatcgccagcactatcagcattgtgaaccagggtctctggctac
 D L A E T V I A S T I S I V N Q V S G Y
 ttcgtgctgggcccaccctatgtgtgtcctggagggtacaccgtctccctgtgtg
 F V L G H P M C V L E G Y T V S L C

EXON 3 (L)

ggatcacagggtctctgggtctctggccatcatttccctgggagagatggatgggtgggtctgcaag
 I T G L W S L A I I S W E R W M V V C K
 ccctttggcaatgtgagatttgatgccaaagctggccatcgtgggcattgccttctcctgg
 P F G N V R F D A K L A I V G I A F S W
 atctgggtctgctgtgtggacagccccgccatctttggttggagcag
 I W S A V W T A P P I F G W S

Exon 4 (L)

gtactggccccacggcctgaagacttcatgcccagacgtgttcagcggcagctcgtac
 Y W P H G L K T S C G P D V F S G S S Y
 cccgggggtgcagtcttacatgattgtcctcatggtcacctgctgcatcatccactcgtc
 P G V Q S Y M I V L M V T C C I I P L A
 atcatcatgctctgctacacctccaagtgtggctggccatccgagcg
 I I M L C Y L Q V W L A I R A

EXON 5 (L)

gtggcaaagcagcagaaaagagtctgaatccaccagaaggcagagaaggaagtgacgcgc
 V A K Q Q K E S E S T Q K A E K E V T R
 atgggtgggtgatgatctttgcgtactgcgtctgctggggaccctacaccttcttcgca
 M V V V M I F A Y C V C W G P Y T F F A
 tgctttgctgctgccaacctggttacgccttccaccctttgatggctgacctgcccggcc
 C F A A A N P G Y A F H P L M A A L P A
 tactttgccaaaagtgcactatctacaacccggtatctatgtctttatgaaccggcag
 Y F A K S A T I Y N P V I Y V F M N R Q

SECOND GENE (M-L HYBRID)**EXON 2 (M)**

gcccttcgaaggcccgaattaccacatcgctcccagatgggtgtaccacctcaccagtgtc
 P F E G P N Y H I A P R W V Y H L T S V
 tggatgatctttgtggtcattgcatccgtcttcacaaatgggcttgtgctggcggccacc
 W M I F V V I A S V F T N G L V L A A T
 atgaagttcaagaagctgcgccaccgctgaactggatcctgggtaacctggcgggtcgct
 M K F K K L R H P L N W I L V N L A V A
 gacctggcagagaccgtcatcgccagcactatcagcgttgtgaaccagggtctatggctac
 D L A E T V I A S T I S V V N Q V Y G Y
 ttcgtgctgggcccaccctatgtgtgtcctggagggtacaccgtctccctgtgtg
 F V L G H P M C V L E G Y T V S L C

EXON 3 (M)

ggatcacaggctctctgggtctctggccatcatttctgggagagatgggtagtggctctgcaag
 I T G L W S L A I I S W E R W V V V C K
 cccttggcaatgtgagatttgatgccaaagctggccatcgtgggcattgccttctcctgg
 P F G N V R F D A K L A I V G I A F S W
 atctgggctgctgtgtggacagccccgccatctttggttggagcaga
 I W A A V W T A P P I F G W S R

Exon 4 (M)

gtactggccccacggcctgaagacttcatgcgcccccagacgtgttcagcggcagctcgtac
 Y W P H G L K T S C G P D V F S G S S Y
 cccggggtgcagctttacatgattgtcctcatggtcacctgctgcatcaccactcagc
 P G V Q S Y M I V L M V T C C I T P L S
 atcatcgtgctctgctacctccaagtgtggctggccatccgagcg
 I I V L C Y L Q V W L A I R A

Exon 5 (L)

gtggcaaagcagcagaaagagtctgaatccaccagaaggcagagaaggaagtgacgcgc
 V A K Q Q K E S E S T Q K A E K E V T R
 atggtggtggtgatgatctttgcgtactgctgtgctggggaccctacaccttcttcgca
 M V V V M I F A Y C V C W G P Y T F F A
 tgctttgctgctgccaaccctggttacgccttccaccctttgatggctgacctgcccggcc
 C F A A A N P G Y A F H P L M A A L P A
 tactttgcaaaaagtgcactatctacaacccgttatctatgtctttatgaaccggcag
 Y F A K S A T I Y N P V I Y V F M N R Q

Table 2. Amino acid sequences for the first and second genes of N29, Da29-1, and Da29-2.

similar separation of 12 nm between L' and L). In an unselected population, carriers with such optimal spacing may be uncommon. We note that the carrier with the second strongest correlation with the anomalous dimension (L / (L + L')) in the MDS test (cDa50) has the same large inferred separation between her pigments. However, a large separation of λ_{\max} does not seem to be sufficient for

exceptional performance on our tests. For example cDa15 has an inferred spectral separation of 11 nm yet does not show unusual performance on the Rayleigh discrimination test or the MDS test. Conversely, cDa20 has an inferred pigment separation of only 4 nm, but she shows a significant correlation with the anomalous dimension (see Table 1) and her son's anomaloscope matching range is small.

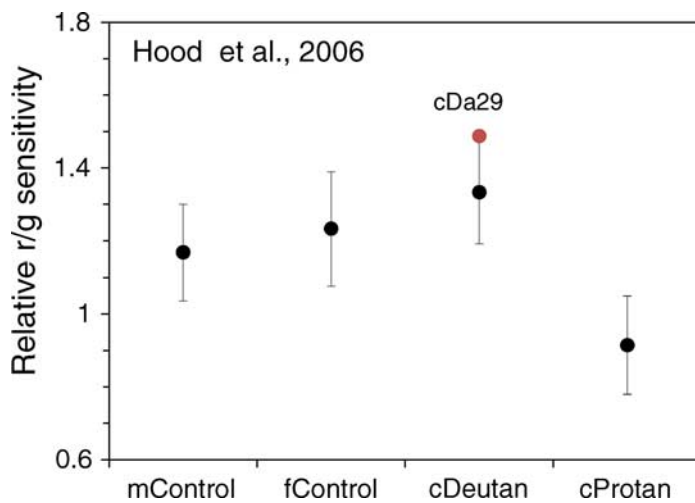


Figure 6. Relative sensitivity to red and green phosphors used by Hood et al. (2006) for two groups of carriers and two control groups. Added as a single participant (red circle) is cDa29, whose relative sensitivity indicates a retinal mosaic that is dominated by cones sensitive to long wavelengths. Error bars are ± 1 standard deviations.

In addition to spectral separation, two other factors must play an important role. The first is the relative number of different types of cone and the weightings given to them by the midget ganglion cells. Cone ratios vary considerably between individuals, and there is some evidence in normals and heterozygotes that color discrimination is poorer when there are disproportionate numbers of L and M cones (Gunther & Dobkins, 2002; Hood, Mollon, Purves, & Jordan, 2006). Deutan carriers specifically are expected to have a greater imbalance of L to M cones (in favor of L cones) and their chromatic discrimination along the L / (L + M) axis in MacLeod Boynton space has been shown to be less precise compared to protan carriers and normal controls (Hood et al., 2006). However, Hood et al. (2006) emphasize that this relatively poorer performance on a single dimension in color space does not rule out the existence of a separate channel that may give weight to the *deuteranomalous* signal and they speculate that this signal may be “most salient in those heterozygotes who have few M cones and for whom the normal L/M signal is weak” (p. 2898). It is of interest here that cDa29 was one of the participants in this earlier study and, although L/M cone ratios were not measured directly, there is a measure of her relative sensitivity to the red and green phosphors used as stimuli in this study (for details, see Hood et al., 2006). cDa29’s performance on their luminance matching test is shown in Figure 6 together with the group data of Hood et al., and it suggests that her cone mosaic is dominated by cones sensitive to long wavelengths: she needed less of the red phosphor to equate luminance when the phosphors were of equal objective luminance for the Judd₁₉₅₁ standard observer (Smith & Pokorny, 1996).

Finally, the optical density of the photopigments should be considered as a possible factor in color discrimination. If a photopigment is present at a low density, its absorption spectrum becomes narrower, owing to the absence of self-screening (Brindley, 1953; Knowles & Dartnall, 1977). It has already been suggested that anomalous trichromats may gain relatively good discrimination by comparing the photon catches in two pigments that have similar λ_{\max} values but different optical densities (He & Shevell, 1995; Neitz, Neitz, He, & Shevell, 1999; Thomas & Mollon, 2004). Similarly, Elsner, Waldvogel, and Burns (1989) found two deuteranomalous observers whose behavior on a color matching task could only be explained by assuming an increased optical density in addition to shifts in their photopigment λ_{\max} values. In this context, we note the substitution of methionine for leucine at site 153 of the long-wave pigment of Da29-1 and Da29-2 (see Table 2): it is conceivable that this substitution alters the effective optical density of the molecule without changing its λ_{\max} .

Given individual variation in spectral separation, cone ratios, and optical densities, we might expect carriers to display varying degrees of behavioral tetrachromacy, according to the relative amplifications of the normal and the anomalous chromatic signals reaching the cortex. In most cases, the “anomalous” signal may be masked by a much stronger L/M signal or may be too weak during ontogeny to recruit an independent subset of post-receptoral channels (Wachtler et al., 2007).

Deuteranomalous color vision affects about 5% of men in Caucasian populations and it is of interest to ask why this anomalous phenotype is maintained. In the case of platyrrhine primates, it is plausible that polymorphic color vision is maintained by a heterozygous advantage to the females, who gain an additional dimension of color discrimination (Mollon et al., 1984). It has sometimes been supposed that a visual advantage to the heterozygotes—e.g., in judging from complexions the fitness of a potential partner or the health of a child—might maintain tetrachromacy in our species (Mollon & Jordan, 1988). However, the rarity of behavioral tetrachromacy suggests that the advantage, if it is to do with color vision, may be to the sons themselves (Bosten et al., 2005).

Conclusions

In summary, among our sample of participants, we have found only one person, a carrier of deuteranomaly, who satisfies the criteria for behavioral tetrachromacy on all our tests. Firstly, she could not make a match on the clinical anomaloscope. Secondly, when asked to discriminate a red/green mixture from a monochromatic orange, there was no combination of $R_{670} / (R_{670} + G_{546})$ and

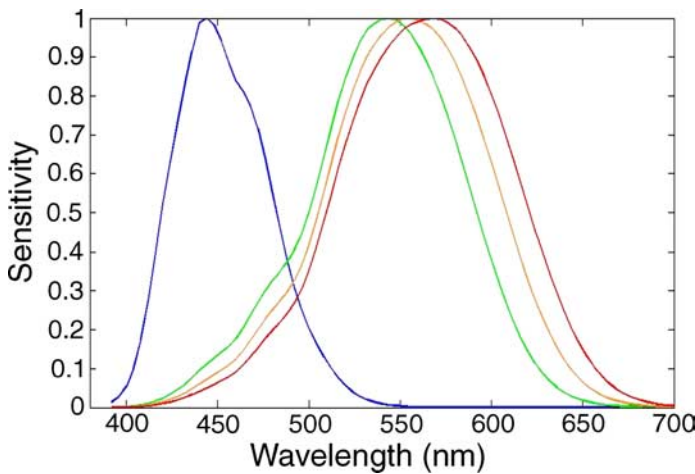


Figure A1. Simulated cone fundamentals for cDa29.

luminance where her responses became either slow or inaccurate. Thirdly, her perceptual color space exhibited the $L / (L + L')$ dimension, which she shares with her deuteranomalous sons. However, while molecular analysis of this participant reveals that she has three well-spaced photopigments in the long-wave spectral region, it is questionable whether this in itself is sufficient to confer strong tetrachromacy.

Appendix A

Modeling MDS performance for our carrier population

Within our sample of carriers, our molecular genetic results show that there are several alleles for the anomalous pigment. This individual variability causes differences in the peak sensitivity of the photopigment molecule. Although we do not know how other factors

(i.e. optical density, lens and macular pigment) might vary in our sample, it is reasonable to expect that individual variation in the peak sensitivity of anomalous and normal photopigments will affect performance on our MDS test. The test was constructed (Bosten et al., 2005) so that pairs of X and Y chips would be metameric for the Smith and Pokorny (1975) normal observer and would be clearly distinguishable by the anomalous observer of DeMarco et al. (1992). For other observers, the two sets of stimuli would be expected to depart from metamerism to a greater or lesser degree. In this Appendix, we assess how well a deuteranomalous signal would separate the X and Y chips in the case of cDa29 and other carriers in our sample.

From each genotyped carrier’s opsin genes, we sought to estimate the peak sensitivity of the M, L, and L’ opsins. There are several strategies by which this can be achieved. Full spectral sensitivities are available from Sharpe et al. (1998), obtained by psychophysical methods from deuteranopes with known hybrid genotypes. But since our candidate tetrachromat’s (cDa29) genotype was not part of their sample, we decided against using these spectral sensitivities.

Instead we simulated cone fundamentals for each of our carriers using the following method: We first used Lamb’s (1995) formula for simulating cone fundamentals of a given peak sensitivity:

$$S(\lambda) = \frac{1}{\{\exp a(A - \frac{\lambda_{max}}{\lambda}) + \exp b(B - \frac{\lambda_{max}}{\lambda}) + \exp c(C - \frac{\lambda_{max}}{\lambda}) + D\}} \tag{A1}$$

where $S(\lambda)$ is the sensitivity of the simulated photopigment as a function of wavelength, $a = 70$, $b = 28.5$, and $c = -14.1$, $A = 0.880$, $B = 0.924$, and $C = 1.104$. We then accounted for self-screening (Brindley, 1953). Since it is not known how anomalous photopigments vary in optical density (see Discussion), we assumed the same value of 0.5 for all photopigments: $S(\lambda) = 1 - 10^{(-0.5 * s(\lambda))}$.

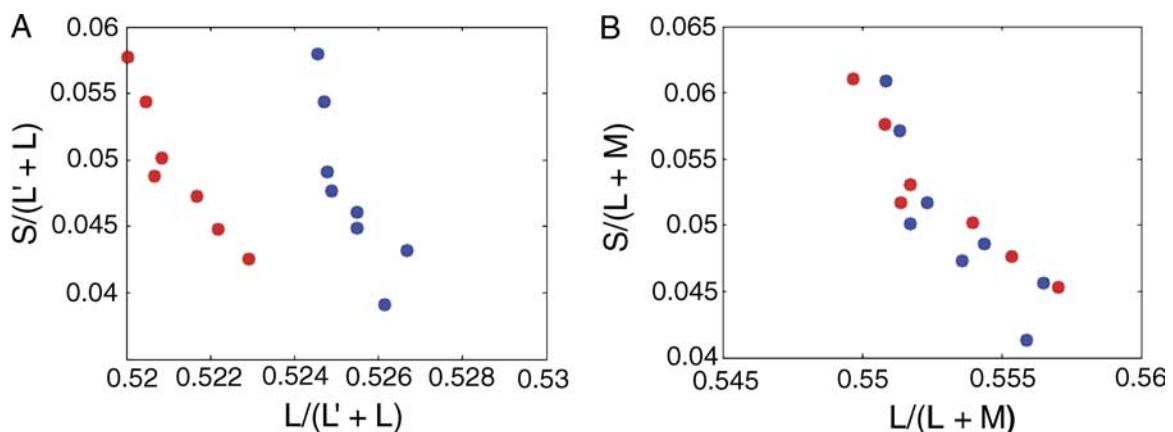


Figure A2. Chromaticities of 15 X and Y stimulus discs modeled in cDa29’s perceptual color space.

We accounted for macular pigment using data provided by Bone et al. (1992) and for lens using data provided by van Norren and Vos (1974).

Two data sets are available for estimating photopigment peak sensitivities from known genotypes. Merbs and Nathans (1992a, 1992b) have estimated the absorption spectra of anomalous and normal photopigments in suspension by photopigment bleaching absorption spectroscopy. Asenjo et al. (1994) have estimated peak sensitivities for various L–M hybrid pigments by a similar method. These two data sets disagree markedly. For example, Merbs and Nathans give the peak sensitivity of the L photopigment with serine at site 180 as 556.7 nm, while Asenjo et al. give it as 563 nm. We tried both data sets in our model but chose the data given by Merbs and Nathans because the reconstructed M and L peak sensitivities corresponded to those of the Smith–Pokorny cone fundamentals (Smith & Pokorny, 1975).

We also simulated a spectral sensitivity curve for the S-cones, assuming that the peak sensitivity of the S photopigment (without correction for pre-receptor filtering and self-screening) was 426.3 nm (Merbs & Nathans, 1992b). Again, our choice was based on the good correspondence to the Smith–Pokorny cone fundamentals (Smith & Pokorny, 1975) used to construct the MDS test. An example of our simulated cone fundamentals (for subject cDa29) is given in Figure A1.

Using cone fundamentals modeled for each carrier, we plotted the positions of our MDS stimuli in a normal chromaticity diagram with the axes L / (L + M) and S / (L + M) and in an analogous anomalous chromaticity diagram with the axes L / (L + L') and S / (L + L'). Our carriers should have access to the signals represented in both chromaticity diagrams. An example of these reconstructed chromaticity diagrams for subject cDa29 is shown in Figure A2.

The X and Y stimulus subsets are separated along L / (L + L') dimensions of all the chromaticity diagrams modeled for our carriers, but not along the normal L / (L + M) dimensions. This is to be expected if the modeled fundamentals approximate the DeMarco et al. (1992) and Smith and Pokorny (1975) fundamentals from which the test was designed. Our modeling predicts that of all our carriers, those with cDa29's genotype should have the most salient L / (L + L') dimension on our MDS test, since this genotype leads to the greatest separation between the X and Y stimulus subsets in our model.

The same model can be used to address the question of whether a woman who is not a carrier for anomalous trichromacy, but who is heterozygous for the serine/alanine polymorphism at site 180 (Winderickx et al., 1992) might show tetrachromacy on our MDS test. We found that for such an observer, the X and Y stimulus subsets are indeed separated along the axis $L_{\text{ser}} / (L_{\text{ser}} + L_{\text{ala}})$, but the size of the difference is less than half of that present along the L / (L + L') axis for cDa29's genotype.

Acknowledgments

This research was supported by the Leverhulme Trust grant F/00125/K (G.J., J.D.M. & S.S.D.), the Wellcome Trust JIF grant 058711/Z/99/Z/LA/ra/ad (G.J.), and the National Institutes of Health grant EY008395 (S.S.D.). We thank N. Atkinson, A. Whitmore, L. Purves, and L. Fu for experimental assistance and W. Smith for programming the dynamic mask.

Commercial relationships: none.

Corresponding author: Gabriele Jordan.

Email: Gabriele.Jordan@ncl.ac.uk.

Address: Newcastle University, Institute of Neuroscience, Henry Wellcome Building, Framlington Place, Newcastle upon Tyne, NE2 4HH, UK.

References

- Asenjo, A. B., Rim, J., & Oprian, D. D. (1994). Molecular determinants of human red/green color discrimination. *Neuron*, *12*, 1131–1138.
- Bone, R., Landrum, J., & Cains, A. (1992). Optical density spectra of the macular pigment in vivo and vitro. *Vision Research*, *32*, 105–110.
- Bosten, J. M., Robinson, J. D., Jordan, G., & Mollon, J. D. (2005). Multidimensional scaling reveals a color dimension unique to 'color-deficient' observers. *Current Biology*, *15*, R950–R952.
- Brindley, G. S. (1953). The effects of colour vision on adaptation to very bright lights. *The Journal of Physiology*, *122*, 332–350.
- Cornsweet, T. N. (1970). *Visual Perception*. New York: Academic Press.
- Dacey, D. M. (1999). Primate retina: Cell types, circuits and color opponency. *Progress in Retinal Eye Research*, *18*, 737–763.
- Deeb, S. S., Hayashi, T., Windericks, J., & Yamaguchi, T. (2000). Molecular analysis of human red/green visual pigment gene locus: Relationship to color vision. *Methods in Enzymology*, *316*, 651–670.
- DeMarco, P., Pokorny, J., & Smith, V. C. (1992). Full-spectrum cone sensitivity functions for X-chromosome-linked anomalous trichromats. *Journal of the Optical Society of America A*, *9*, 1465–1476.
- De Vries, H. (1948). The fundamental response curves of normal and abnormal dichromatic and trichromatic eyes. *Physica*, *14*, 367–380.
- Elsner, A. E., Waldvogel, J., & Burns, S. A. (Eds.) (1989). *High illuminance color matching in anomalous*

- trichromacy* (vol. IX). Dordrecht: Kluwer Academic Publishers.
- Franceschetti, A. (1928). Die Bedeutung der Einstellungsbreite am Anomaloskop für die Diagnose der einzelnen Typen der Farbensinnstörungen, nebst Bemerkungen über ihren Vererbungsmodus. *Schweizerische Medizinische Wochenschrift*, *52*, 1273–1279.
- Gunther, K. L., & Dobkins, K. R. (2002). Individual differences in chromatic (red/green) contrast sensitivity are constrained by the relative number of L- versus M-cones in the eye. *Vision Research*, *42*, 1367–1378.
- Hayashi, T., Motulsky, A. G., & Deeb, S. S. (1999). Position of a ‘green-red’ hybrid gene in the visual pigment array determines colour-vision phenotype. *Nature Genetics*, *22*, 90–93.
- He, J. C., & Shevell, S. K. (1995). Variation in color matching and discrimination among deuteranomalous trichromats: Theoretical implications of small differences in photopigments. *Vision Research*, *35*, 2579–2588.
- Hood, S. M., Mollon, J. D., Purves, L., & Jordan, G. (2006). Color discrimination in carriers of color deficiency. *Vision Research*, *46*, 2894–2900.
- Jacobs, G. H., Williams, G. A., Cahill, H., & Nathans, J. (2007). Emergence of novel color vision in mice engineered to express a human cone photopigment. *Science*, *315*, 1723–1725.
- Jordan, G., & Mollon, J. D. (1993). A study of women heterozygous for color deficiencies. *Vision Research*, *33*, 1495–1508.
- Knowles, A., & Dartnall, H. J. A. (1977). *The eye* (vol. 2B). New York: Academic Press.
- Kruskal, J. B. (1964). Multidimensional scaling by optimizing goodness of fit to a nonmetric hypothesis. *Psychometrika*, *29*, 1–27.
- Lamb, T. (1995). Photoreceptor spectral sensitivities: Common shape in the long-wavelength region. *Vision Research*, *35*, 3083–3091.
- Lennie, P., Haake, P. W., & Williams, D. R. (1991). The design of chromatically opponent receptive fields. In M. S. Landy & J. A. Movshon (Eds.), *Computational models of visual processing* (pp. 71–82). Cambridge, MA: MIT Press.
- Linsker, R. (1990). Perceptual neural organization: Some approaches based on network models and information theory. *Annual Review of Neuroscience*, *13*, 257–281.
- Lyon, M. F. (1961). Gene action in the X-chromosome of the mouse (*Mus musculus* L.). *Nature*, *190*, 372–373.
- MacLeod, D. I. A. (1985). Receptor constraints on colour appearance. In D. Ottoson & S. Zeki (Eds.), *Central and peripheral mechanisms of colour vision* (pp. 103–116). London: MacMillan.
- MacLeod, D. I. A., & Boynton, R. M. (1979). Chromaticity diagram showing cone excitation by stimuli of equal luminance. *Journal of the Optical Society of America*, *69*, 1183–1186.
- Merbs, S. L., & Nathans, J. (1992a). Absorption spectra of the hybrid pigments responsible for anomalous color vision. *Science*, *258*, 464–466.
- Merbs, S. L., & Nathans, J. (1992b). Absorption spectra of human cone pigments. *Nature*, *356*, 433–435.
- Mollon, J. D. (1997). ‘...aus dreierley Arten von Membranen oder Molekülen’: George Palmer’s legacy. In C. R. Cavonius (Ed.), *Colour vision deficiencies: XIII* (pp. 3–20). Dordrecht: Kluwer.
- Mollon, J. D., Bowmaker, J. K., & Jacobs, G. H. (1984). Variations of colour vision in a New World primate can be explained by polymorphism of retinal photopigments. *Proceedings of the Royal Society of London B*, *222*, 373–399.
- Mollon, J. D., & Jordan, G. (1988). Eine evolutionäre Interpretation des menschlichen Farbensehens. *Die Farbe*, *35/36*, 139–170.
- Nagy, A. L., MacLeod, D. I., Heyneman, N. E., & Eisner, A. (1981). Four cone pigments in women heterozygous for color deficiency. *Journal of the Optical Society of America*, *71*, 719–722.
- Nathans, J., Piantanida, T. P., Eddy, R. L., Shows, T. B., & Hogness, D. S. (1986). Molecular genetics of inherited variation in human color vision. *Science*, *232*, 203–232.
- Neitz, J., Neitz, M., He, J. C. A., & Shevell, S. K. (1999). Trichromatic color vision with only two spectrally distinct photopigments. *Nature Neuroscience*, *2*, 884–888.
- Oda, S., Ueyama, H., Nishida, Y., Tanabe, S., & Yamada, S. (2003). Analysis of L-cone/M-cone visual pigment gene arrays in females by long-range PCR. *Vision Research*, *43*, 489–495.
- Pokorny, J., Smith, V. C., Verriest, G., & Pinckers, A. J. L. G. (1979). *Congenital and acquired color vision defects*. New York: Grune & Stratton.
- Rayleigh, L. (1881). Experiments on colour. *Nature*, *25*, 64–66.
- Regan, B. C., Reffin, J. P., & Mollon, J. D. (1994). Luminance noise and the rapid determination of discrimination ellipses in colour deficiency. *Vision Research*, *34*, 1279–1299.
- Rodieck, R. W. (1977). Metric of color borders. *Science*, *197*, 1195–1196.

- Sharpe, L. T., Stockman, A., Jägle, H., Knau, H., Klaussen, G., Reitner, A., et al. (1998). Red, green, and red-green hybrid pigments in the human retina: Correlations between deduced protein sequences and psychophysically measured spectral sensitivities. *Journal of Neuroscience*, *18*, 10053–10069.
- Shepard, R. N. (1962). The analysis of proximities: Multidimensional scaling with an unknown distance function. *Psychometrika*, *27*, 219–246.
- Shevell, S., He, J. C., Kainz, P., Neitz, J., & Neitz, M. (1998). Relating color discrimination to photopigment genes in deutan observers. *Vision Research*, *38*, 3371–3376.
- Smith, V. C., & Pokorny, J. (1975). Spectral sensitivity of the foveal cone photopigments between 400 and 500 nm. *Vision Research*, *15*, 161–171.
- Smith, V. C., & Pokorny, J. (1996). The design and use of a cone chromaticity space: A tutorial. *Color Research and Application*, *21*, 375–383.
- Teplitz, R. L. (1965). Sex chromatin of cone cells of human retina. *Science*, *150*, 1828–1829.
- Thomas, P. B., & Mollon, J. D. (2004). Modelling the Rayleigh match. *Visual Neuroscience*, *21*, 477–482.
- van Norren, D., & Vos, J. (1974). Spectral transmission of the human ocular media. *Vision Research*, *14*, 1237–1244.
- Waalder, G. H. M. (1927). Über Erblichkeitsverhältnisse der verschiedenen Arten von angeborener Rotgrünblindheit. *Zeitschrift für induktive Abstammungs- und Vererbungslehre*, *45*, 279–333.
- Wachtler, T., Doi, E., Lee, T.-W., & Sejnowski, T. J. (2007). Cone selectivity derived from the responses of the retinal cone mosaic to natural scenes. *Journal of Vision*, *7*(8):6, 1–14, <http://www.journalofvision.org/content/7/8/6>, doi:10.1167/7.8.6. [PubMed] [Article]
- Winderickx, J., Lindsey, D. T., Sanocki, E., Teller, D. Y., Motulsky, A. G., & Deeb, S. S. (1992). A Ser/Ala polymorphism in the red photopigment underlies variation in colour matching among colour-normal individuals. *Nature*, *356*, 431–433.